Organic Process Research & Development

Article

pubs.acs.org/OPRD

Intermittent Simulated Moving Bed Processes for Chromatographic Three-Fraction Separation

Simon Jermann, Shigeharu Katsuo,[‡] and Marco Mazzotti*

ETH Zurich, Institute of Process Engineering, Sonneggstrasse 3, CH-8092 Zurich, Switzerland

ABSTRACT: Simulated moving bed (SMB) chromatography is a well-established technique to resolve racemic mixtures into pure enantiomers. However, the conventional SMB process is restricted to binary separations, and its applicability is therefore limited when impurities are present. In this contribution we address this issue by considering impurities as a third fraction which is separated from the two product streams, i.e. the pure enantiomers, by two novel intermittent SMB (I-SMB) concepts. The process schemes studied consist of four sections, each section comprising only one column, and are straightforward extensions of the original I-SMB process; therefore, the switch time is also divided into two substeps. Substep I is characterized by feed and withdrawal of two product streams, whereas in substep II only pure solvent is introduced to the unit in order to recover the third product stream and to adjust the relative positions of the concentration fronts along the column train. The two concepts presented in this contribution differ in the column configuration and in the withdrawal of the product streams. One process is characterized by withdrawal of the most retained component during substep II, whereas in the other process the least retained species is recovered in the second substep. Consequently, these processes are termed 3S-ISMB and 3W-ISMB, respectively. These process schemes are analyzed in the frame of equilibrium theory under the assumption of linear chromatographic conditions, thus yielding a graphical representation of the region of complete ternary separation similar to classical triangle theory. Furthermore, an experimental study of the 3W-ISMB concept is presented in which a ternary system consisting of a mixture of the enantiomers of γ-phenyl-γ-butyrolactone and of the (−)-Tröger's Base enantiomer (the impurity in this context) is separated in pure ethanol on the chiral stationary phase Chiralpak AD. These experiments are carried out under linear chromatographic conditions, namely the concentration of each solute is kept constant at 0.5 g/L. A purity of at least 94% for all product streams is achieved, which demonstrates successfully the potential of this novel, three-fraction SMB-like process.

1. INTRODUCTION

Simulated moving bed (SMB) chromatography has been around for roughly 50 years now and was originally designed in the oil industry as a large-scale process for two-fraction separations.[1,2] Later on its application scope was extended to the sugar industry[3] before being adapted in the 1990s by the pharmaceutical industry for manufacturing chiral and biological drugs.[4] The latter development triggered increased research activities in the field, and various modifications of the original SMB process have been reported.[4] Most of these new SMB-like processes are, however, still restricted to two-fraction separations, thus limiting their applicability to the case of the separation of enantiomers in the presence of impurities or of the purification of biological compounds.

In the recent past a number of research groups have been addressing this issue with the aim of developing multicolumn processes that allow for ternary or even quaternary separations.[5−15] These processes can be roughly classified into two groups, namely continuous process schemes with a large number of columns and semicontinuous processes characterized by a relatively small number of columns.

It is worth discussing the process schemes proposed so far in more detail. A straightforward solution to achieve ternary separation is the coupling of two standard SMB units either via the extract or the raffinate stream of the first unit; such SMB cascades were proposed by Wankat and co-workers.[5,6] A similar alternative is obtained by combining two units into one bigger unit with internal recycle, the so-called integrated SMB unit consisting of eight or nine zones.[7−10] The 3F-SMB process proposed earlier[16] uses a five-zone SMB in which the most retained component is trapped inside the column and carried backwards with the simulated movement of the solid until it is eventually eluted by applying a stronger eluent. This process is only feasible, however, if the selectivity between the intermediate component and the most retained one is rather high. An alternative approach using a five-zone SMB has been recently reported by Mun[11] where alternate opening and closing of the product ports facilitates feasibility for a broader range of ternary systems. All of these process schemes belong to the group of continuous processes, in the sense that the feed and the products are continuously introduced into or withdrawn from the unit.

Important semicontinuous alternatives are the two-zone SMB/chromatography hybrid system,[12] the JO process,[13,14] and the multicolumn countercurrent solvent gradient purification (MCSGP).[15] Interestingly reports about experimental studies on these three-fraction SMB-like processes are rather rare in the open literature. In this paper we follow the semicontinuous approach and present two four-column intermittent SMB schemes that are extensions of the semicontinuous I-SMB process;[17,18] moreover we also demonstrate the potential of these new process schemes experimentally. In

Special Issue: INTENANT

Received: August 31, 2011
Published: January 9, 2012

 © 2012 American Chemical Society dx.doi.org/10.1021/op200239e | *Org. ProcessRes. Dev.* 2012, 16, 311−322

section 2 it is shown how I-SMB can be exploited to allow for ternary separations, which results in two novel process schemes. In addition, purity constraints for these new process schemes are developed. This is followed by an experimental study on the separation of a ternary system consisting of a mixture of the enantiomers of γ-phenyl-γ-butyrolactone and the (−)-Tröger's Base enantiomer (the impurity) in pure ethanol on Chiralpak AD (section 3 and section 4).

2. THEORY AND PROCESS SCHEMES

In order to better understand the development of the new ternary separation processes it is worth recalling briefly the principle of I-SMB (see Figure 1). Similarly to standard SMB,

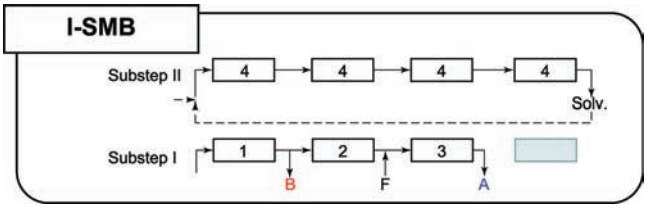

Figure 1. Process scheme of closed loop intermittent simulated moving bed (I-SMB) chromatography. Feed (F) supply and withdrawal of raffinate (A) and extract (B) is conducted in substep I, whereas in substep II all inlet and outlet ports are closed.

the I-SMB unit consists of four zones; however, in contrast to SMB the switch period is divided into two substeps. In substep I the unit is operated as an SMB without flow in section 4; in substep II all inlet and outlet ports are closed, and the fluid is just circulated through the column train in order to adjust the relative position of the concentration profiles. It has been shown that I-SMB in 1-1-1-1 configuration doubles the productivity of 1-2-2-1 standard SMB whilst fulfilling high-purity specifications.[17,18] This feature allows us to restrict the following discussion on processes in 1-1-1-1 configuration, i.e. on four-column processes. Furthermore, we note that we avoid using the term section since it is not as clearly defined for the intermittent processes as compared to standard SMB. Hence, we refer to the column positions instead of referring to sections.

From Figure 1 it becomes apparent that in the case of a feed consisting of three species, A, B and C, the I-SMB process can be adapted to allow for three-fraction separation by withdrawing an additional product stream in substep II. In principle one can collect either the most retained component (C) or the least retained component (A) during the second substep. The former approach will be referred to as 3S-ISMB as it is a three-fraction I-SMB process characterized by withdrawal of the strongest component in substep II. Accordingly, the alternative scheme is termed 3W-ISMB. Both approaches can be analyzed in the frame of equilibrium theory under linear chromatographic conditions; they are discussed separately in the following two subsections.

2.1. 3S-ISMB. A schematic of the 3S-ISMB scheme is shown in Figure 2, where the only modification with respect to the standard I-SMB is an additional outlet in substep II. The separation of the two weaker adsorbing components (A and B) is based on exactly the same principle as in I-SMB. The strongest retained component (C), in contrast, is just trapped inside the column and carried backwards with the simulated movement of the solid until it is eventually eluted from the

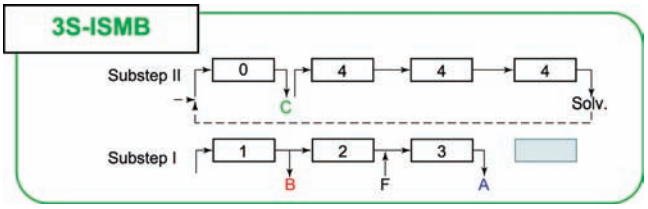

Figure 2. Process scheme of 3S-ISMB which follows directly from I-SMB and is characterized by an additional product stream, namely withdrawal of the most retained component (C) in substep II.

column occupying the first position in substep II, thus allowing for the regeneration of the solid phase.

In order to develop constraints for complete ternary separation, the propagation of the adsorption front and desorption tail of each component of the ternary mixture to be separated needs to be analyzed. In the frame of equilibrium theory under linear chromatographic conditions, the propagation velocity of species i in the SMB zone j, ν_j^i, is given by

$$\nu_j^i = \frac{u_j/\varepsilon^*}{1 + \nu H_i} \tag{1}$$

where H_i is the Henry's constant of component i, u_j is the superficial velocity in section j, and ν is the phase ratio, i .e $\nu = (1 - \varepsilon^*)/\varepsilon^*$, ε^* being the overall void fraction. Let us first apply eq 1 to species A, which is collected during substep I at the end of the third column. In order to fulfill the separation requirements, the adsorption front of A should not reach the end of the fourth column during substep II, and the desorption tail of A should completely leave the second column during substep II. These considerations are represented graphically in the physical plane where coordinates are the time and the space coordinate along the unit's columns, as shown in Figure 3. In the figure each species corresponds to a different color, and its propagation takes place along straight characteristics, whose slope is given by the reciprocal of the velocity in eq 1. The following constraints are obtained:

$$\nu_4^{\mathrm{A}} t^*_{\mathrm{II}} \le L_c \tag{2a}$$

$$L_c \le \nu_2^{\mathrm{A}} t^*_{\mathrm{I}} + \nu_4^{\mathrm{A}} t^*_{\mathrm{II}} \tag{2b}$$

where L_c is the column length, t^*_{I} and t^*_{II} are the durations of substeps I and II, respectively. Noteworthy, the requirement for A leaving the third column in the raffinate stream, i.e. $L_c \le \nu_3^{\mathrm{A}} t^*_{\mathrm{I}} + \nu_4^{\mathrm{A}} t^*_{\mathrm{II}}$, is implicitly included in eq 2a as $\nu_3^{\mathrm{A}} \ge \nu_2^{\mathrm{A}}$.

For the sake of convenience, we multiply eqs 2a and 2b by the column's cross-sectional area A and replace the term Au_j by Q_j, Q_j being the volumetric flow rate as indicated in Figure 2, thus yielding:

$$\frac{Q_4 t^*_{\mathrm{II}}}{\varepsilon^*(1 + \nu H_{\mathrm{A}})} \le V \tag{3a}$$

$$V \le \frac{Q_2 t^*_{\mathrm{I}}}{\varepsilon^*(1 + \nu H_{\mathrm{A}})} + \frac{Q_4 t^*_{\mathrm{II}}}{\varepsilon^*(1 + \nu H_{\mathrm{A}})} \tag{3b}$$

where V is the column volume. Let us introduce the following dimensionless flow rate ratios m_j and reduced Henry's constants $\tilde{H}_i$:

dx.doi.org/10.1021/op200239e | Org. ProcessRes. Dev. 2012, 16, 311−322

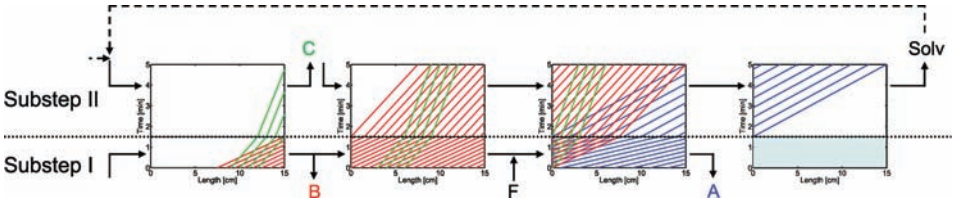

Figure 3. Physical plane for 3S-ISMB where coordinates are the time and the space coordinate along the unit's columns. Each species propagates along straight characteristics, the slope of which is given by the reciprocal of the velocity in eq 1. The blue characteristics represent species A, the red characteristics, species B, and the green ones, species C. The dotted line divides the time axis in substeps I and II.

$$m_j = \frac{t^*_j Q_j}{V\varepsilon^*} \tag{4a}$$

$$\tilde{H}_i = 1 + \nu H_i \tag{4b}$$

where t^*_j is the duration of the substep associated to flow rate j, namely $t^*_j = t^*_{\mathrm{I}}$ for j = 1,2,3 and $t^*_j = t^*_{\mathrm{II}}$ for j = 0,4 . Then eqs 3a and 3b can be recast simply as:

$$m_4 \le \tilde{H}_{\mathrm{A}} \tag{5a}$$

$$\tilde{H}_{\mathrm{A}} \le m_2 + m_4 \tag{5b}$$

Analogous considerations for the adsorption fronts and desorption tails of the other two components yield the following full set of constraints for complete ternary separation in a 3S-ISMB unit:

$$m_4 \le \tilde{H}_{\mathrm{A}} \tag{6a}$$

$$\tilde{H}_{\mathrm{A}} \le m_2 + m_4 \tag{6b}$$

$$m_3 + m_4 \le \tilde{H}_{\mathrm{B}} \tag{6c}$$

$$\tilde{H}_{\mathrm{B}} \le m_1 + m_4 \tag{6d}$$

$$m_1 + m_2 + m_3 + 2m_4 \le \tilde{H}_{\mathrm{C}} \tag{6e}$$

$$\tilde{H}_{\mathrm{C}} \le m_1 + m_2 + 2m_4 + m_0 \tag{6f}$$

These constraints are further simplified by transforming the dimensionless flow rate ratios m_j into a set of combined flow rate ratios $\hat{m}_j$ as defined in the following equations:

$$\hat{m}_0 \equiv m_0 \tag{7a}$$

$$\hat{m}_1 \equiv m_1 + m_4 \tag{7b}$$

$$\hat{m}_2 \equiv m_2 + m_4 \tag{7c}$$

$$\hat{m}_3 \equiv m_3 + m_4 \tag{7d}$$

$$\hat{m}_4 \equiv m_4 \tag{7e}$$

It is worth noting that these combined flow rate ratios $\hat{m}_j$ lose the physical meaning which is usually associated to the flow rate ratios m_j; these definitions are in fact driven by the structure of the physical constraints given in eqs 6a−6f. With this transformation, eqs 6a−6f reduce to the following simple inequalities:

$$\hat{m}_4 \le \tilde{H}_{\mathrm{A}} \tag{8a}$$

$$\tilde{H}_{\mathrm{A}} \le \hat{m}_2 \tag{8b}$$

$$\hat{m}_3 \le \tilde{H}_{\mathrm{B}} \tag{8c}$$

$$\tilde{H}_{\mathrm{B}} \le \hat{m}_1 \tag{8d}$$

$$\hat{m}_1 + \hat{m}_2 + \hat{m}_3 - \hat{m}_4 \le \tilde{H}_{\mathrm{C}} \tag{8e}$$

$$\tilde{H}_{\mathrm{C}} \le \hat{m}_1 + \hat{m}_2 + \hat{m}_0 \tag{8f}$$

These constraints can be represented graphically in the $(\hat{m}_2, \hat{m}_3)$ plane (see Figure 4), where eqs 8b and 8c define a triangular region within which complete separation of A and B can be achieved. It is worth noting that eq 8f can always be independently fulfilled by choosing $\hat{m}_0$ appropriately. Furthermore there is always a feasible range for $\hat{m}_4$; hence, eq 8a is

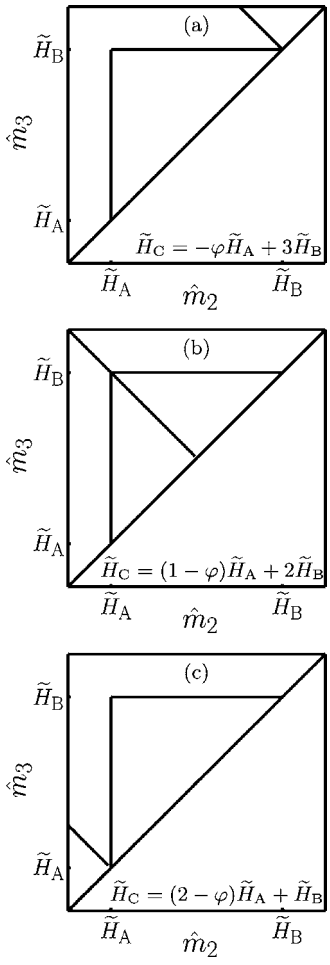

Figure 4. Triangular region of complete separation for 3S-ISMB in the $(\hat{m}_2, \hat{m}_3)$ plane and critical line $(\hat{m}_3 \le -\hat{m}_2 + \tilde{H}_{\mathrm{C}} - \tilde{H}_{\mathrm{B}} + \varphi\tilde{H}_{\mathrm{A}})$ below which complete ternary separation is feasible. The critical line is shown for three different values of $\tilde{H}_{\mathrm{C}}$ and subfigure (c) shows that the process becomes infeasible if $\tilde{H}_{\mathrm{C}} \le (2-\varphi)\tilde{H}_{\mathrm{A}} + \tilde{H}_{\mathrm{B}}$.

dx.doi.org/10.1021/op200239e | Org. ProcessRes. Dev. 2012, 16, 311−322

conveniently replaced by

$$\hat{m}_4 \equiv \varphi \tilde{H}_A \tag{9}$$

where $0 \leq \varphi \leq 1$. However, the constraints on $\hat{m}_1$ defined by eqs 8d and 8e are of a different nature . The lower bound on $\hat{m}_1$ depends on $\tilde{H}_B$ only, whereas the upper bound depends on $\tilde{H}_C$ as well as on $\hat{m}_2$, $\hat{m}_3$, and $\hat{m}_4$, which becomes clear by recasting eqs 8d and 8e as:

$$\tilde{H}_B \leq \hat{m}_1 \leq \tilde{H}_C - \hat{m}_2 - \hat{m}_3 + \hat{m}_4 \tag{10}$$

Therefore, a feasible range of $\hat{m}_1$ values only exists when the upper bound in eq 10 is larger than the lower bound, i.e. when the operating point in the $(\hat{m}_2, \hat{m}_3)$ plane is chosen below a critical straight line with negative slope given by the linear inequality

$$\hat{m}_3 \leq -\hat{m}_2 + \tilde{H}_C - \tilde{H}_B + \varphi \tilde{H}_A \tag{11}$$

The triangular region of complete separation together with the critical line defined by eq 11 is shown in Figure 4 for three systems with different selectivities. It is noted that these plots only provide information on the feasibility of the process and on the choice of the operating point in the $(\hat{m}_2, \hat{m}_3)$ plane. For the full region of complete separation a three-dimensional (3D) plot in the space $(\hat{m}_1, \hat{m}_2, \hat{m}_3)$ for a fixed value of φ would be required. For the sake of brevity we do not show the corresponding 3D plots but note only that the 3D region of complete separation becomes larger as φ increase, which leads, however, to a higher solvent consumption.

At this point it is worth commenting on the feasibilty of the 3S-ISMB concept depending on the selectivities of the components to be separated. From eq 11 and Figure 4 it can be readily seen that the 3S-ISMB process becomes infeasible if the critical line intersects the diagonal at $(\tilde{H}_A, \tilde{H}_A)$ or below. Feasibility of the process is therefore solely determined by the y-axis intersect of the critical line, i.e. the term $\tilde{H}_C - \tilde{H}_B + \varphi \tilde{H}_A$. Furthermore, it is obvious that the relative position of the critical line with respect to the triangular region shifts downwards if the selectivities between the most retained component and the other two species decrease. If these selectivities reach a value that causes the critical line to intersect the diagonal at $(\tilde{H}_A, \tilde{H}_A)$, no feasible operating points in the $(\hat{m}_2, \hat{m}_3)$ plane can exist. Therefore, we conclude that the 3S-ISMB process becomes infeasible if

$$\tilde{H}_C \leq (2 - \varphi)\tilde{H}_A + \tilde{H}_B \tag{12}$$

This result is in accordance with previous studies on the five-zone 3F-SMB process[16] mentioned above, as expected since the separation is based on very similar principles. To overcome this difficulty an alternative process has been developed and is presented in the next subsection.

2.2. 3W-ISMB. As already mentioned above, it is also possible to collect the weakest adsorbing component during the second substep. This requires, however, more modifications to the original I-SMB process than in the 3S-ISMB case. With reference to Figure 5 it is to be noted that contrary to I-SMB (see Figure 1), in a 3W-ISMB process, all four columns are in use during substep I. Columns 1 and 2 are disconnected from the column train in order to elute the strong component C and the intermediate component B, respectively. The remaining columns are connected in series and fed with the mixture to be separated. After substep I, column 1 is completely regenerated and is not used in the second substep; the remaining three

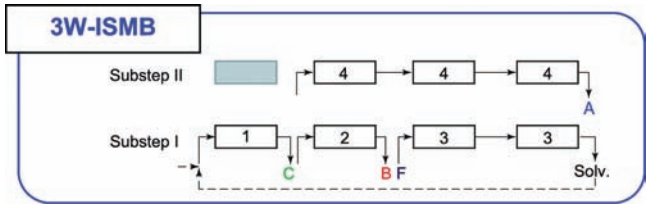

Figure 5. Process scheme of 3W-ISMB which is characterized by withdrawal of the least retained component (A) in substep II.

columns are connected in series and fed with pure eluent in order to adjust the relative position of the composition fronts and to elute component A. The purity constraints for 3W-ISMB were derived in the same manner as for 3S-ISMB (see section 2.1). The propagation paths of the different species in the physical plane are illustrated in Figure 6. The same definitions for dimensionless flow rate ratios and reduced Henry's constants, given in eqs 4a and 4b, apply. Therefore, another set of six inequalities can be obtained as given by:

$$m_3 \leq \tilde{H}_A \tag{13a}$$

$$\tilde{H}_A \leq m_4 \tag{13b}$$

$$m_3 + m_4 \leq \tilde{H}_B \tag{13c}$$

$$\tilde{H}_B \leq m_2 + m_4 \tag{13d}$$

$$m_2 + m_3 + m_4 \leq \tilde{H}_C \tag{13e}$$

$$\tilde{H}_C \leq \begin{cases} m_1 + m_2 + m_4 & (\tilde{H}_C \leq m_2 + m_3 + 2m_4) \\ m_1 + m_2 + 2m_4 & (\tilde{H}_C > m_2 + m_3 + 2m_4) \end{cases} \tag{13f}$$

These equations are slightly more complicated than the ones for 3S-ISMB (eqs 6a−6f) as two different cases have to be considered to describe the behavior of the tail of the most retained component. Also these constraints can be simplified by transforming the flow rate ratios m_j into a set of combined flow rate ratios:

$$\hat{m}_1 \equiv m_1 + m_2 + m_4 \tag{14a}$$

$$\hat{m}_2 \equiv m_2 + m_4 \tag{14b}$$

$$\hat{m}_3 \equiv m_2 + m_3 + m_4 \tag{14c}$$

$$\hat{m}_4 \equiv m_4 \tag{14d}$$

Note that the combined flow rate ratios are defined differently than in the case of the 3S-ISMB process (eqs 7a−7e) because of the different structure of eq 13e with respect to eq 6e. Applying the combined flow rate ratios defined above, eqs 13a−13f reduce to

$$\hat{m}_3 - \hat{m}_2 \leq \tilde{H}_A \tag{15a}$$

$$\tilde{H}_A \leq \hat{m}_4 \tag{15b}$$

$$\hat{m}_3 - \hat{m}_2 + \hat{m}_4 \leq \tilde{H}_B \tag{15c}$$

$$\tilde{H}_B \leq \hat{m}_2 \tag{15d}$$

dx.doi.org/10.1021/op200239e | Org. ProcessRes. Dev. 2012, 16, 311−322

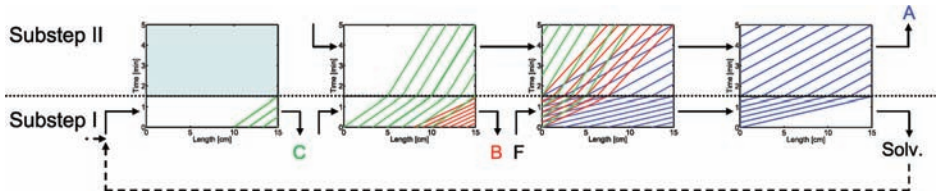

Figure 6. Physical plane for 3W-ISMB where coordinates are the time and the space coordinate along the unit's columns. Each species propagates along straight characteristics, whose slope is given by the reciprocal of the velocity in eq 1. The blue characteristics represent species A, the red characteristics, species B, and the green ones, species C. The dotted line divides the time axis into substeps I and II.

$$\hat{m}_3 \le \tilde{H}_C \tag{15e}$$

$$\tilde{H}_C \le \begin{cases} \hat{m}_1 & (\tilde{H}_C \le \hat{m}_3 + \hat{m}_4) \\ \hat{m}_1 + \hat{m}_4 & (\tilde{H}_C > \hat{m}_3 + \hat{m}_4) \end{cases} \tag{15f}$$

These equations can be represented graphically in the $(\hat{m}_2, \hat{m}_3)$ plane (see Figure 7). Equations 15d and 15e define a right triangular region of complete separation, whilst eqs 15a and 15c can be combined to obtain two equations for a critical line, namely

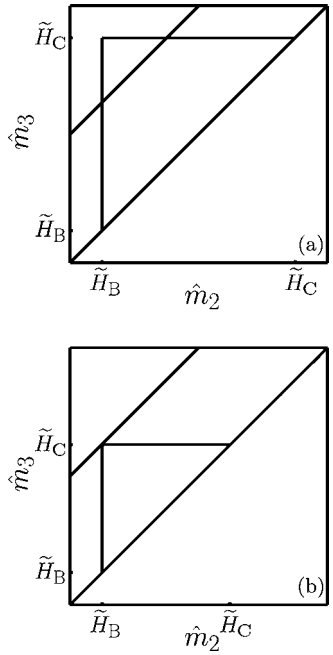

Figure 7. Triangular region of complete separation for 3W-ISMB in the $(\hat{m}_2, \hat{m}_3)$ plane together with the critical line. In the case of 3W-ISMB the critical line has a positive slope which renders the process feasible for any combination of $\tilde{H}_i$-values. The critical line is independent of $\tilde{H}_C$; therefore, it does not intersect the triangular region below a certain selectivity between component B and C (see subfigure b); i.e. in these cases the region of complete separation is determined by $\tilde{H}_B$ and $\tilde{H}_C$ only.

$$\hat{m}_3 \le \hat{m}_2 + \tilde{H}_A \tag{16a}$$

$$\hat{m}_3 \le \hat{m}_2 + \tilde{H}_B - \hat{m}_4 \tag{16b}$$

Similarly to 3S-ISMB we replace $\hat{m}_4$ with

$$\hat{m}_4 \equiv \frac{\tilde{H}_A}{\varphi} \tag{17}$$

where $0 \le \varphi \le 1$; hence, the equation for the critical line simplifies to

$$\hat{m}_3 \le \hat{m}_2 + \min\left(\tilde{H}_A, \tilde{H}_B - \frac{\tilde{H}_A}{\varphi}\right) \tag{18}$$

This means that the critical line, below which complete ternary separation is feasible, is parallel to the diagonal in the $(\hat{m}_2, \hat{m}_3)$ plane and that complete ternary separation is always feasible. However, the region of complete separation can become very narrow if the selectivity between the weak and the intermediate component is small. Finally, it is noteworthy that the whole triangular region becomes accessible if

$$\tilde{H}_C \le \begin{cases} \tilde{H}_A + \tilde{H}_B & \left(\left(1 + \frac{1}{\varphi}\right)\tilde{H}_A \le \tilde{H}_B\right) \\ 2\tilde{H}_B - \frac{\tilde{H}_A}{\varphi} & \left(\left(1 + \frac{1}{\varphi}\right)\tilde{H}_A > \tilde{H}_B\right) \end{cases} \tag{19}$$

as shown in Figure 7b.

2.3. Extra-Column Dead Volume in the 3W-ISMB Unit.

In section 3 an experimental study on the 3W-ISMB process is presented which was carried out on a lab-scale 3W-ISMB unit. In lab-scale units the extra-column dead volume can easily be of the same order of magnitude as the column volume and thus not be negligible. Therefore it is necessary to revise the purity constraints developed above in order to explicitly account for the increase in residence time due to the additional dead volume. For the sake of brevity we will derive these additionl constraints only for 3W-ISMB as we are only reporting experimental data for this process.

In previous publications it has been shown that the extra-column dead volume can be accounted for, both in conventional SMB[19,20] as well as in I-SMB units[18] by using an effective flow ratio $\bar{m}_j$ which is defined as

$$\bar{m}_j = m_j - m_j^D = \frac{t^*_s Q_j}{V\varepsilon^*} - \frac{V_j^D}{V\varepsilon^*} \tag{20}$$

where $\bar{m}_j$ is the effective flow rate ratio in section j, V_j^D is the extra-column dead volume in section j, and m_j^D is defined as $m_j^D = V_j^D/(V\varepsilon^*)$.

It has been shown that the same purity constraints defined by "Triangle Theory"[21] apply in small-scale units when m_j is replaced by $\bar{m}_j$.[19,20] However, in a 3W-ISMB unit the situation is different since the fluid in a large part of the extra-column dead volume, namely the tubing from the outlet manifold to the inlet manifold of the next column, remains stagnant when the column is disconnected from the column train. Therefore, we have to impose additional constraints especially on the fronts and tails of the strongest retained component.

dx.doi.org/10.1021/op200239e | Org. ProcessRes. Dev. 2012, 16, 311–322

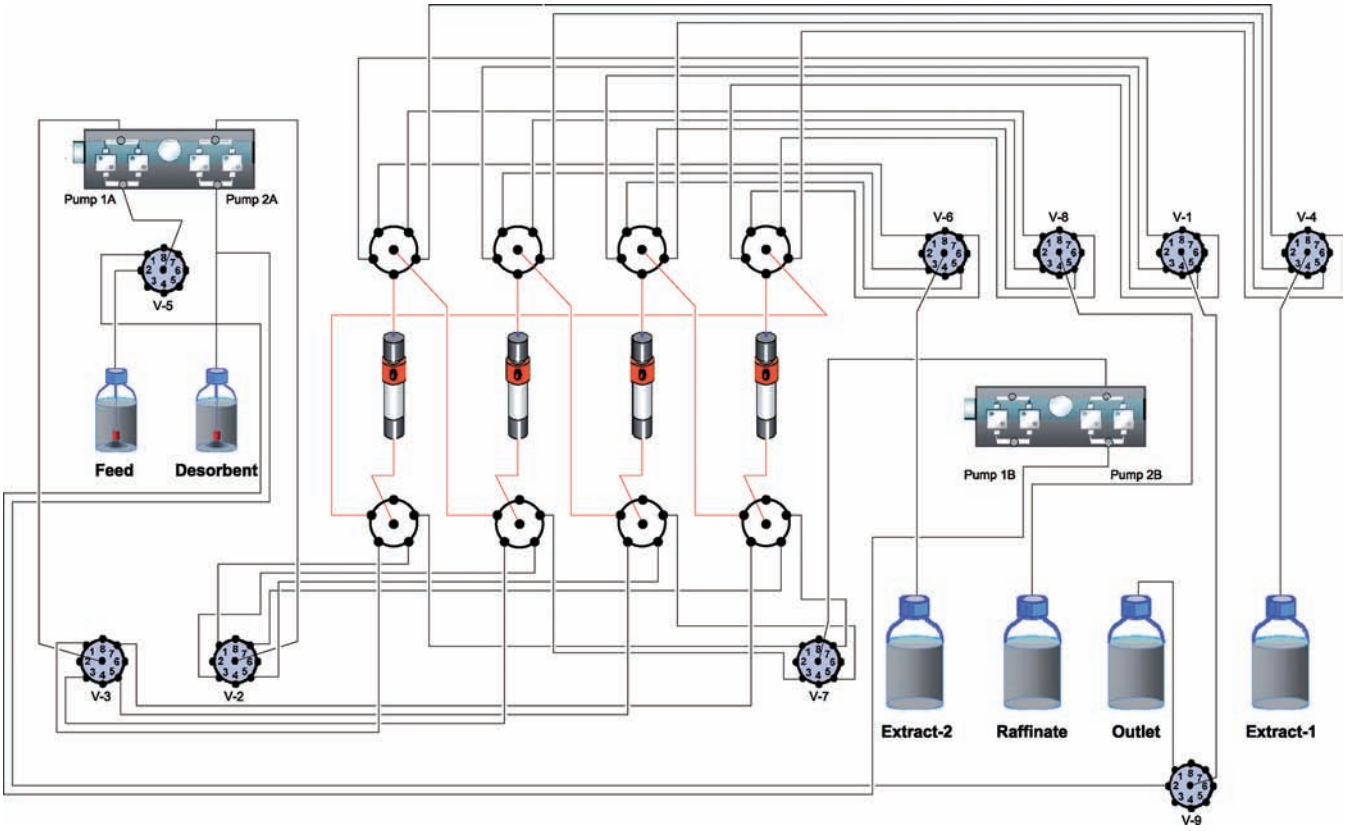

Figure 8. Flowsheet of the experimental setup consisting of two binary gradient pumps, four chromatographic columns equipped with inlet and outlet manifolds, and nine multiposition valves.

With reference to Figure 6 it is noted that in the derivation of the 3W-ISMB constraints above where extra-column dead volume is neglected, component C is allowed to break through column 2 during substep II and into column 3. However, as the tubing between outlet manifold of column 2 and inlet manifold of column 3 remains stagnant for the following two switches, any quantity of component C entering this part of the tubing would remain there until this particular tubing becomes reconnected to the column train, i.e. when the column has moved to position 3. Once this happens, any residue of component C would enter column 4, thus spoiling the purity of either the raffinate or the extract-2 stream. In order to prevent such pollution, it is necessary to impose a more stringent constraint on the front of C, so as to avoid breakthrough of component C from column 2. As a result, a condition similar to the case of 3S-ISMB is obtained, namely that C is trapped in the column and just carried backwards until it is eluted from column 1. In the case of 3S-ISMB this condition rendered complete ternary separation infeasible for low selectivity systems, the same situation can therefore occur in 3W-ISMB if the extra-column dead volume is strictly taken into account, as shown in detail in Appendix.

For the remaining part of this contribution we explicitly relax these stringent constraints and allow component C to break through column 2. By doing so, we guarantee that there is a feasible operating region for the process, but we also expect some pollution from component C in extract-2 originating from the temporarily stagnant part of the tubing. Nonetheless, we account for extra-column effects by introducing effective flow rate ratios $\bar{m}_j$, which we define as:

$$\bar{m}_1 \equiv m_1 + m_2 + m_4 - m_2^{\mathrm{D}} \tag{21a}$$

$$\bar{m}_2 \equiv m_2 + m_4 - m_1^{\mathrm{D}} \tag{21b}$$

$$\bar{m}_3 \equiv m_2 + m_3 + m_4 - m_2^{\mathrm{D}} \tag{21c}$$

$$\bar{m}_4 \equiv m_4 - m_1^{\mathrm{D}} \equiv \frac{\tilde{H}_{\mathrm{A}}}{\varphi} \tag{21d}$$

with

$$m_1^{\mathrm{D}} = \frac{V_1^{\mathrm{D}}}{V\varepsilon^*} \tag{22a}$$

$$m_2^{\mathrm{D}} = \frac{V_2^{\mathrm{D}}}{V\varepsilon^*} \tag{22b}$$

where V_1^{D} represents the total extra-column dead volume between two successive column, i.e. the tubing between inlet manifold and column inlet, between column outlet and outlet manifold, and from the outlet manifold to the inlet manifold of the next column; whereas V_2^{D} includes the tubing between inlet manifold and column inlet as well as the tubing from the column outlet to the outlet manifold.

dx.doi.org/10.1021/op200239e | Org. ProcessRes. Dev. 2012, 16, 311–322

The critical line (eq 18) can be recast as:

$$\bar{m}_3 \le \bar{m}_2 + \min\left(\tilde{H}_A + 2m_1^D - m_2^D, \tilde{H}_B - \frac{\tilde{H}_A}{\varphi} + m_1^D - m_2^D\right) \quad (23)$$

For more details on the derivation of eqs 21−23 the reader is referred to the Appendix.

3. EXPERIMENTAL SECTION

3.1. Experimental Setup. The experimental setup for the 3W-ISMB process is based on a modified ÄKTA explorer 100 system (GE Healthcare Europe GmbH, Freiburg, Germany).[22] The program controlling all the devices is based on the standard UNICORN software (GE Healthcare Europe GmbH, Freiburg, Germany). The experiments were carried out in a 1-1-1-1 open loop configuration.

The laboratory unit was set up according to the flowsheet shown in Figure 8. The inlet and outlet manifolds connect the columns to the multiposition valves which are needed to control the different streams in the unit and to realize the periodic switching of the columns. Three multiposition valves are connected to the inlet manifolds and to the pumps delivering feed and solvent, respectively. Another four multiposition valves are connected to the outlet manifolds in order to collect the three product streams and the regenerated solvent stream from the outlet port. Finally two additional valves allow for switching between open- and closed-loop configuration (V-9) and for switching from feed solution to pure solvent (V-5) for cleaning the unit. Note that this setup can be implemented easily on an existing SMB unit as no additional pumps are required, namely only two additional multiposition valves with the corresponding tubing are necessary to accommodate an additional inlet and outlet stream .

As discussed above in section 2.3 the extra-column dead volume plays a crucial role in lab-scale SMB units and consists of three different tubing parts. Namely from the inlet manifold to the column inlet (V_a = 0.03 mL), from the column outlet to the outlet manifold (V_b = 0.02 mL) and from the outlet manifold to the inlet manifold of the following column (V_c = 0.18 mL). The volumes of these tubing parts have been determined very precisely using 1,3,5-tris-*tert*-butylbenzene (TTBB) as a tracer, the details being reported elsewhere.[18,20] Using these values, V_1^D and V_2^D are equal to 0.23 and 0.05 mL, respectively.

3.2. Materials. This work studies the separation of a mixture consisting of racemic γ-phenyl-γ-butyrolactone (Sigma-Aldrich Chemie GmbH, Buchs, Switzerland) and the (−)-Tröger's Base enantiomer in pure ethanol (analytical grade, Scharlab S.L., Sentmenat, Spain) on Chiralpak AD (Chiral Technologies Europe, Illkirch, France). It is noted that the pure (−)-Tröger's Base enantiomer was obtained previously by separating a racemic mixture of Tröger's Base (Sigma-Aldrich Chemie GmbH, Buchs, Switzerland) using a conventional SMB process according to a procedure reported elsewhere.[23] The model system was then prepared by dissolving 106.12 mg of the as-prepared (−)-Tröger's Base (component C) and 204.25 mg γ-phenyl-γ-butyrolactone racemate (components A and B) in 156.82 g ethanol, i.e. the concentration of all three solutes was 0.5 g/L; the chromatogram of this mixture is shown in Figure 9.

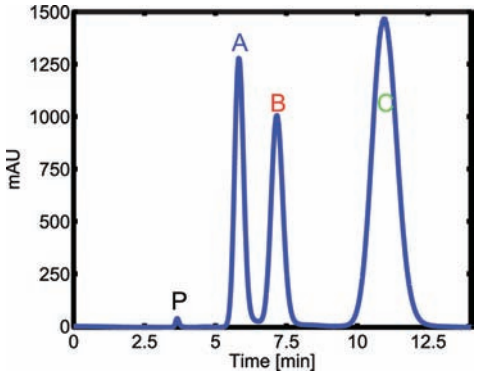

Figure 9. Experimental model system consisting of racemic γ-phenyl-γ-butyrolactone (denoted by A and B) and the (−)-Tröger's Base enantiomer (C) in pure ethanol separated on Chiralpak AD (Q = 0.5 mL/min, $c_{F,i}$ = 0.5 g/L); P denotes the injection peak.

The Chiralpak AD stainless steel columns (15 cm × 0.46 cm, 20 μm particle size) were prepacked by the manufacturer and were used for the separation in the 3W-ISMB unit as well as for analytical purposes. Namely, the product streams were analyzed on a Dionex Ultimate 3000 HPLC unit (Sunnyvale, CA, U.S.A.) using the same mobile phase as in the preparative application. The overall void fraction, ε*, of each column was determined by injecting 1,3,5-tris-*tert*-butylbenzene (Sigma-Aldrich Chemie GmbH, Buchs, Switzerland), which is considered to be nonretained, according to the following equation

$$\varepsilon^* = \frac{t_0 Q}{V} \quad (24)$$

where V is the column volume, Q is the applied flow rate, and t_0 is the residence time of a nonretained species.

3.3. Linear Adsorption. The Henry's constants of the three solutes, i.e. γ-phenyl-γ-butyrolactone (species A and B) and (−)-Tröger's Base (species C), were determined by measuring the retention time of a diluted pulse injection according to the relationship

$$H_i = \frac{\varepsilon^*}{1-\varepsilon^*}\frac{t_{R,i} - t_0}{t_0} \quad (i = A, B, C) \quad (25)$$

where H_i is the Henry's constant of solute i and $t_{R,i}$ is the retention time of solute i (i = A,B,C). It is further noted that t_0 and $t_{R,i}$ were corrected with the dead time of the HPLC unit. All experiments were carried out at T = 23 ± 1 °C. The system characteristics are reported in Table 1.

Table 1. System characteristics

Column			
A [cm^2]			0.166
L [cm]			15
ε^* [−]			0.68
ΔP_{max} [bar]			40
	Component		
linear isotherm	(±)-γ-phenyl-γ-butyrolactone		(−)-Tröger's Base
H_i	1.58	2.49	5.41
$\tilde{H}_i$	1.74	2.17	3.54

dx.doi.org/10.1021/op200239e | Org. ProcessRes. Dev. 2012, 16, 311−322

3.4. Operating Point. Using the values given in Table 1 and analyzing the system in the frame of the theory explained in section 2, it becomes clear that complete ternary separation of this model system is only feasible in a 3W-ISMB unit with negligible extra-column dead volume (Figure 10a) and becomes infeasible for the 3S-ISMB process (see Figure 10b). It is further noted, that a strict consideration of extra-column effects according to Appendix A.1 renders also 3W-ISMB on our lab-scale unit infeasible. Nevertheless we implemented the 3W-ISMB concept on our unit in order to prove the purity constraints developed above and to demonstrate the potential of this technology for large-scale applications where the extra-column dead volume would be negligible and the process would be feasible.

The operating point for 3W-ISMB in terms of $\bar{m}_j$-values as defined in eqs 21a−21d can be chosen graphically as shown in Figure 11a. Once the operating point in the $(\bar{m}_2, \bar{m}_3)$ plane is selected, the duration of substeps I and II, i.e. t^*_s, needs to be determined in order to calculate the actual flow rates Q_j. This can be done by solving an optimization problem that aims at maximizing the feed throughput at minimal switch time and minimal solvent consumption under the following constraints: the selected $\bar{m}_j$-values are applied and the maximum allowable pressure drop in the columns cannot be overcome. Such an optimization problem can be formulated as follows:

$$\begin{aligned}
&\underset{Q_j, t^*_s}{\text{minimize}} \quad [-\lambda_F Q_3 t^*_I + \lambda_S (Q_1 + Q_2) t^*_I \\
&\qquad\qquad + \lambda_S Q_4 t^*II + \lambda_t (t^*_I + t^*_{II})] \\
&\text{subject to} \quad \frac{L}{A}\phi Q_1 - \Delta P_{max} \le 0 \\
&\qquad \frac{L}{A}\phi Q_2 - \Delta P_{max} \le 0 \\
&\qquad 2\frac{L}{A}\phi Q_3 - \Delta P_{max} \le 0 \\
&\qquad 3\frac{L}{A}\phi Q_4 - \Delta P_{max} \le 0 \\
&\qquad \bar{m}_1 = \frac{t^*_I Q_1}{V\varepsilon^*} + \frac{t^*_I Q_2}{V\varepsilon^*} + \frac{t^*_{II} Q_4}{V\varepsilon^*} - m_2^D \\
&\qquad \bar{m}_2 = \frac{t^*_I Q_2}{V\varepsilon^*} + \frac{t^*_{II} Q_4}{V\varepsilon^*} - m_1^D \\
&\qquad \bar{m}_3 = \frac{t^*_I Q_2}{V\varepsilon^*} + \frac{t^*_I Q_3}{V\varepsilon^*} + \frac{t^*_{II} Q_4}{V\varepsilon^*} - m_2^D \\
&\qquad \bar{m}_4 = \frac{t^*_{II} Q_4}{V\varepsilon^*} - m_1^D
\end{aligned} \tag{26}$$

where L and A are the column length and cross-section area, respectively, ΔP_{max} is the maximum allowable pressure drop, λ_F, λ_S, and λ_t are weighting factors for the different elements of the objective function. Finally, ϕ is the pressure drop factor according to Darcy's law, i.e.

$$\phi = \frac{\Delta P_j A}{Q_j L} \tag{27}$$

For the sake of simplicity, we have solved the optimization problem (eq 26) only for the first experimental run, i.e. run α,

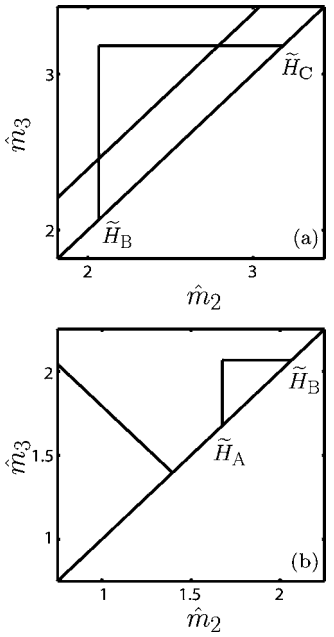

Figure 10. Graphical analysis of the model system according to Table 1. Triangle and critical line for complete separation are shown for both the 3W-ISMB process (a) and the 3S-ISMB process (b). In both cases the upper limit of $\varphi = 1$ was chosen, and the extra-column dead volume was neglected. Moreover, (b) shows that 3S-ISMB is infeasible for this model system.

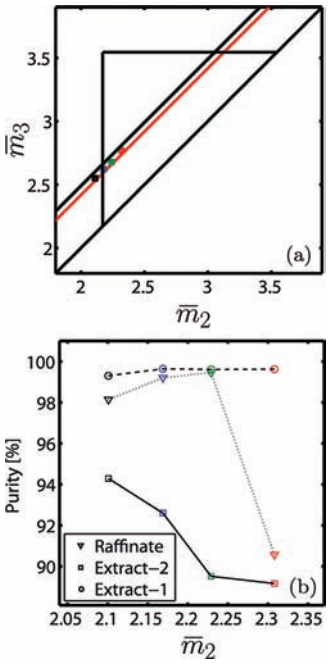

Figure 11. (a) Operating point of the four experimental runs α−δ represented in the $(\bar{m}_2, \bar{m}_3)$ plane. Two critical lines are shown; the one in red applies for run α only, whereas the black one applies for runs β−δ. The upward shift is due to a smaller value of $\bar{m}_4$. (b) Purity of the three product streams plotted against the $\bar{m}_2$-value of the operating point.

and we have kept the substep durations constant for the subsequent runs, i.e. runs β−δ. The substep durations were determined as t^*_I = 1.50 min and t^*_{II} = 3.98 min, the corresponding flow rates for the four experimental runs are

dx.doi.org/10.1021/op200239e | Org. ProcessRes. Dev. 2012, 16, 311−322

reported in Table 2 together with the graphically selected $\bar{m}_j$-values.

Table 2. Operating conditions for the experimental runs $\alpha-\delta$ with substep durations of 1.50 min for substep I and 3.98 min for substep II

	flow rate (mL/min)				flow rate ratio			
run	Q_1	Q_2	Q_3	Q_4	$\bar{m}_1$	$\bar{m}_2$	$\bar{m}_3$	$\bar{m}_4$
α	1.31	0.52	0.39	0.85	3.59	2.32	2.77	1.86
β	1.92	0.51	0.38	0.82	4.04	2.24	2.68	1.79
γ	2.00	0.44	0.38	0.82	4.05	2.18	2.62	1.79
δ	2.06	0.36	0.38	0.82	4.04	2.11	2.55	1.79

4. RESULTS AND DISCUSSION

The compositions and the purities of the three product streams at cyclic steady state for the four operating points reported in Table 2 are given in Table 3. The purities are defined as:

$$Pu_i = \frac{c_i}{c_A + c_B + c_C} \tag{28}$$

where i = A for the purity of the raffinate (the stream where the less retained enantiomer of γ-phenyl-γ-butyrolactone is collected), i = B for extract-2 (the stream where the more retained enantiomer of γ-phenyl-γ-butyrolactone is collected), and i = C for extract-1 (the stream where (−)-Tröger's Base is collected).

Furthermore, Figure 11 shows the position of the operating points in the ($\bar{m}_2$, $\bar{m}_3$) plane as well as the purities of all product streams as a function of $\bar{m}_2$. In the following, the experimental performance of these runs is discussed with reference to the theoretical design criteria for 3W-ISMB presented in section 2.3.

With reference to Figure 11a we note that we decreased the $\bar{m}_4$-value from run α to run β and kept it constant for the following two runs, i.e. runs γ and δ. Therefore two critical lines are shown in Figure 11a, namely the red line belonging to run α and the black line belonging to the other three runs. It is further noted that the operating point α lies above the critical line, whereas operating points β to δ lie below it.

Since the position of the operating point with respect to the critical line determines the purity of the raffinate, pollution of the raffinate from component B for run α is expected, whereas a pure raffinate should be obtained in runs $\beta-\delta$. In Figure 11b the triangles representing the raffinate purity clearly illustrate that the purity of run α is indeed significantly lower as compared to those of the other three runs which are close to purity. The small fluctuations of the purities in runs $\beta-\delta$ are attributed to the fact that the operating points lie very close to the critical line, i.e. a small shift of either the operating point due to flow rate fluctuations or the boundaries due to temperature fluctuations can cause a decrease in the raffinate purity. Nonetheless, we can state that the general trends as shown in Figure 11b are in good agreement with the prediction from theory.

Provided that the lower bound for $\bar{m}_4$ is not violated, the purities of extract-1 and extract-2 depend on the position of the operating point with respect to the triangle only. We note that the vertical line of the triangle marks the boundary for the extract-1 purity, i.e. an operating point to the left of that boundary leads to pollution from component B in extract-1, whereas an operating point above the horizontal line results in a polluted extract-2.

Figure 11 shows that the general trends for the purities of extract-1 and extract-2 are in good agreement with theory. Namely we observe an extract-1 purity of 99.6% for runs $\alpha-\gamma$ and a slightly lower purity for run δ, whose corresponding operating point lies outside the triangle of complete separation.

The purity of extract-2 increases steadily from 89.2% (run α) to 94.3% (run δ), which is in agreement with theory since the operating point moves away from the horizontal boundary of the triangle. However, as the operating points lie well inside the region of complete separation, a much higher purity would be expected. There are two main reasons for such an unexpected low purity of extract-2, namely the pollution caused by component C stemming from the temporarily stagnant part of the extra-column tubing and the axial dispersion, which is not accounted for in triangle theory. The latter needs some further discussion since the effect of dispersion is much more prominent in 3W-ISMB as compared to that in standard SMB.

Dispersive effects are causing more relative pollution in 3W-ISMB units because of a different internal concentration profile. Any quantity of component B entering the unit in column 3 is eluted after one switch from the same column, i.e. when it is in position 2. This requires not only baseline separation between A and B but also results, for the feed concentrations studied, in the formation of a component B peak that has the Gaussian shape typical of column chromatography. As a consequence, the relative pollution due to dispersion is much more significant than in standard SMB where an internal concentration profile with large plateaus characteristic of countercurrent operations is built up and where we know that axial dispersion has a minor effect.

Furthermore, it is noted that dispersion causes pollution of extract-2 from both components A and C as shown in Table 3. As expected, the decrease of $\bar{m}_4$ from run α to run β causes an increased pollution from component A, although the overall purity gets better because moving away from the horizontal boundary results in lower pollution from C which compensates for the larger amount of A polluting extract-2. In the following runs γ and δ, $\bar{m}_4$ was kept constant; hence, no change in the relative amount of A was observed. Therefore, the shift downwards to the left causes a significant increase in the overall extract-2 purity, as less and less C is present in extract-2.

Table 3. Concentrations of all three solutes in the outlet streams and corresponding product purities for runs $\alpha-\delta$

	raffinate - A				extract-2 - B				extract-1 - C			
run	c_A [g/L]	c_B [g/L]	c_C [g/L]	Pu (%)	c_A [g/L]	c_B [g/L]	c_C [g/L]	Pu (%)	c_A [g/L]	c_B [g/L]	c_C [g/L]	Pu (%)
α	0.0835	0.0084	0.0004	90.6	0.0068	0.3292	0.0332	89.2	0.0002	0.0003	0.1237	99.6
β	0.0886	0.0002	0.0003	99.5	0.0126	0.3702	0.0308	89.5	0.0002	0.0002	0.0931	99.6
γ	0.0922	0.0004	0.0003	99.2	0.0150	0.4436	0.0206	92.6	0.0003	0.0000	0.0950	99.6
δ	0.0697	0.0013	0.0000	98.1	0.0169	0.4754	0.0119	94.3	0.0002	0.0004	0.0889	99.3

dx.doi.org/10.1021/op200239e | Org. ProcessRes. Dev. 2012, 16, 311−322

5. CONCLUSION

In this contribution two intermittent four columns SMB processes for ternary separations have been presented. In both processes the switch time is divided into two substeps, i.e. a first substep during which the feed is introduced to the unit and the second substep without feeding. The main difference between the two processes is the sequence of product withdrawal. One process is characterized by withdrawal of the most retained component during the second substep, whilst the other two product streams are collected during substep I. In the other process presented, the least retained component is collected during substep II, consequently the most retained and the intermediate retained component are withdrawn in the first substep. Due to this difference the processes were termed 3S-ISMB and 3W-ISMB, respectively.

Both 3S-ISMB and 3W-ISMB have been analyzed in the frame of equilibrium theory. For both processes a region of complete ternary separation similar to the classical triangle theory could be derived. This analysis revealed that on the one hand 3W-ISMB always allows for complete ternary separation no matter what combinations of Henry's constants characterize the ternary mixture to separate. On the other hand 3S-ISMB becomes infeasible if the selectivity between the intermediate and the most retained component is not large enough. Furthermore we have discussed the effect of extra-column dead volume which becomes very important in small-scale SMB units where the volume of the tubing between the columns is of the same order of magnitude as the column volume. For 3W-ISMB we have shown that additional constraints are necessary when the extra-column dead volume is non-negligible and that these additional constraints may also lead to situations where complete ternary separation becomes infeasible.

After analyzing the two processes theoretically, a model system for experimental validation has been presented which consists of a mixture of the enantiomers of γ-phenyl-γ-butyrolactone and the (−)-Tröger's Base enantiomer in pure ethanol on the CSP Chiralpak AD. Analysis of the model system chosen revealed that both 3S-ISMB and 3W-ISMB with non-negligible extra-column dead volume were infeasible, whereas 3W-ISMB with negligible extra-column dead volume is always feasible. Therefore, we have chosen 3W-ISMB for experimental validation, although we could only demonstrate its potential on a small-scale unit where complete ternary separation is not possible due to extra-column effects.

In the Experimental Section we have shown that 3W-ISMB can be easily implemented on an existing SMB unit by making only a few modifications and most importantly by requiring no additional pumps. Furthermore, our experimental results for this process have proven the applicability of the modified triangle theory for ternary separation. In addition the potential of the new process has been demonstrated successfully; we were able to obtain purities of at least 94% for all three product streams despite the fact that our small-scale unit does not allow for complete ternary separation. This is a result of both axial dispersion and non-negligible extra-column dead volume effects. In contrast to standard SMB the latter effect cannot be eliminated completely due to a periodic switch between disconnected and interconnected mode. As far as axial dispersion is concerned, a much more significant effect occurs in 3W-ISMB as compared to standard SMB, since the intermediate retained component (B) has an internal concentration profile with Gaussian shape normally occurring in column chromatography where we know that axial dispersion is much more prominent than in countercurrent operation. Therefore, column efficiency is of more concern in 3W-ISMB than in SMB.

APPENDIX

Extra-Column Dead Volume in the 3W-ISMB Unit

In section 2.3 we discussed the effect of extra-column dead volume in the small-scale 3W-ISMB unit and state that the process can become infeasible when extra-column dead volume effects are strictly taken into account. In the following we substantiate that claim and furthermore present a less stringent approach that accounts for the dead volume by only introducing effective flow rate ratios (eqs 21a and 21b) without changing the structure of the ideal case (eqs 13a−13f).

Strict Constraints

In order to prevent breakthrough of component C in column 2 and to account for the increased residence time due to extra-column tubing the following constraints are necessary:

$$m_3 - m_1^{\mathrm{D}} \le \tilde{H}_{\mathrm{A}} \tag{29a}$$

$$\tilde{H}_{\mathrm{A}} \le m_4 - m_1^{\mathrm{D}} \tag{29b}$$

$$m_3 + m_4 - m_1^{\mathrm{D}} \le \tilde{H}_{\mathrm{B}} \tag{29c}$$

$$\tilde{H}_{\mathrm{B}} \le m_2 + m_4 - m_1^{\mathrm{D}} \tag{29d}$$

$$m_2 + m_3 + 2m_4 - m_2^{\mathrm{D}} \le \tilde{H}_{\mathrm{C}} \tag{29e}$$

$$\tilde{H}_{\mathrm{C}} \le m_1 + m_2 + 2m_4 - m_2^{\mathrm{D}} \tag{29f}$$

where m_1^{D} and m_2^{D} are given in eqs 22a and 22b. It is worth pointing out that a distinction of cases in eq 29f is no longer necessary due to eq 29e which, in fact, means that the most retained component (C) has to be trapped in the column and carried backwards with the simulated movement of the solid until it reaches column 1, i.e. a condition similar to 3S-ISMB. It is therefore to be expected that the adoption of eq 29e may also render the 3W-ISMB process infeasible for certain low-selectivity systems.

With reference to eqs 29a−29f we transform the dimensionless flow rate ratios m_j in order to obtain simple relationships in the combined flow rate ratios $\hat{m}_j$ as above. For 3W-ISMB with non-negligible extra-column dead volume we therefore define $\hat{m}_j$ as

$$\hat{m}_1 \equiv m_1 + m_2 + 2m_4 - m_2^{\mathrm{D}} \tag{30a}$$

$$\hat{m}_2 \equiv m_2 + m_4 - m_1^{\mathrm{D}} \tag{30b}$$

$$\hat{m}_3 \equiv m_2 + m_3 + 2m_4 - m_2^{\mathrm{D}} \tag{30c}$$

$$\hat{m}_4 \equiv m_4 - m_1^{\mathrm{D}} \equiv \frac{\tilde{H}_{\mathrm{A}}}{\varphi} \tag{30d}$$

and end up with a new set of constraints that reads

$$\hat{m}_3 - \hat{m}_2 - \hat{m}_4 - 3m_1^{\mathrm{D}} + m_2^{\mathrm{D}} \le \tilde{H}_A \tag{31a}$$

$$\tilde{H}_{\mathrm{A}} \le \hat{m}_4 \tag{31b}$$

$$\hat{m}_3 - \hat{m}_2 - 2m_1^{\mathrm{D}} + m_2^{\mathrm{D}} \le \tilde{H}_{\mathrm{B}} \tag{31c}$$

$$\tilde{H}_{\mathrm{B}} \le \hat{m}_2 \tag{31d}$$

dx.doi.org/10.1021/op200239e | Org. ProcessRes. Dev. 2012, 16, 311−322

$$\hat{m}_3 \le \tilde{H}_C \tag{31e}$$

$$\tilde{H}_C \le \hat{m}_1 \tag{31f}$$

As for the case with negligible extra-column dead volume we obtain a right triangle in the $(\hat{m}_2, \hat{m}_3)$ plane defined by eqs 31d and 31e, whereas eqs 31a and 31c define a critical line below which complete ternary separation is feasible. This critical line is given by

$$\hat{m}_3 \le \hat{m}_2 + \min\left(\left(1 + \frac{1}{\varphi}\right)\tilde{H}_A + 3m_1^D - m_2^D, \tilde{H}_B + 2m_1^D - m_2^D\right) \tag{32}$$

From the definition of $\hat{m}_2$ and $\hat{m}_3$ given in eqs 30b and 30c, respectively, it is evident that the line corresponding to a zero feed flow rate is not the diagonal as usual but a straight line parallel to the diagonal given by

$$\hat{m}_3 = \hat{m}_2 + \frac{\tilde{H}_A}{\varphi} + 2m_1^D - m_2^D \tag{33}$$

Consequently 3W-ISMB with non-negligible extra-column dead volume becomes infeasible when the band between the zero-feed-line (eq 33) and the critical line ((eq 32) does not cross the triangular region of complete separation (eqs 31c and 31d), which occurs when

$$\tilde{H}_C - \tilde{H}_B < \frac{\tilde{H}_A}{\varphi} + 2m_1^D - m_2^D$$

Effective Flow Rate Ratios

For the ternary system studied in section 3 the strict consideration of the extra-column dead volume as outlined above, renders the process infeasible. Therefore we apply an alternative approach that explicitly considers the increased residence time due to extra-column tubing, but neglects the effect of stagnant flow in some parts of tubing, i.e. we relax the stringent constraint on the front of C (eq 29e and allow component C to break through column 2. The full set of constraints thus reads as:

$$m_3 - m_1^D \le \tilde{H}_A \tag{34a}$$

$$\tilde{H}_A \le m_4 - m_1^D \tag{34b}$$

$$m_3 + m_4 - m_1^D \le \tilde{H}_B \tag{34c}$$

$$\tilde{H}_B \le m_2 + m_4 - m_1^D \tag{34d}$$

$$m_2 + m_3 + m_4 - m_2^D \le \tilde{H}_C \tag{34e}$$

$$\tilde{H}_C \le m_1 + m_2 + m_4 - m_2^D \tag{34f}$$

Applying the effective flow rate ratios $\bar{m}_j$ defined in eqs 21a to 21d these constraints simplify to:

$$\bar{m}_3 - \bar{m}_2 - 2m_1^D + m_2^D \le \tilde{H}_A \tag{35a}$$

$$\tilde{H}_A \le \bar{m}_4 \tag{35b}$$

$$\bar{m}_3 - \bar{m}_2 + \bar{m}_4 - m_1^D + m_2^D \le \tilde{H}_B \tag{35c}$$

$$\tilde{H}_B \le \bar{m}_2 \tag{35d}$$

$$\bar{m}_3 \le \tilde{H}_C \tag{35e}$$

$$\tilde{H}_C \le \bar{m}_1 \tag{35f}$$

and thus the critical line as given in eq 23 is obtained by combining eqs 35a to 35c.

AUTHOR INFORMATION

Corresponding Author

*E-mail: marco.mazzotti@ipe.mavt.ethz.ch. Telephone: +41 44 632 24 56. Fax: +41 44 632 11 41.

Present Address

‡Mitsubishi Chemical Group Science and Technology Research Center, Inc., 1000 Kamoshidacho, Aoba-ku, Yokohama 227-8502, Japan.

ACKNOWLEDGMENTS

This work is a contribution to the research project INTENANT, funded by the European Commission within the seventh Framework Programme (Project No. 214 129).

NOTATION

$f'(c)$	derivative of the adsorption isotherm with respect to c
H_i	Henry's constant of component i [−]
$\tilde{H}_i$	reduced Henry's constant of component i [−]
L_c	column length [cm]
m	dimensionless flow rate ratio [−]
$\hat{m}$	combined dimensionless flow rate ratio [−]
$\bar{m}$	effective flow rate ratio [−]
ΔP	pressure drop [bar]
Pu	purity [%]
Q	volumetric flow rate [mL/min]
t	time [min]
t^*_s	duration of substeps [min]
t_0	residence time of a nonretained species [min]
T	temperature [°C]
V	column volume [mL]
V_j^D	dead volume [mL]
y	axis intersect for the critical line in 3W-ISMB [−]
z	spacial coordinate [cm]

Subscripts and Superscripts

D	dead volume
F	feed
i	component index (i = A,B,C)
j	flow rate index (j = 0,1,2,3,4)
max	maximum
R	retention
S	solvent
s	substep index (s = I,II)
t	time

Greek symbols

ε^*	overall void fraction [−]
λ	weighting factors [−]
ν	phase ratio [−]
ϕ	pressure drop factor [bar min/cm^2]
φ	parameter in 3S-ISMB and 3W-ISMB ($0 \le \varphi \le 1$) [−]

dx.doi.org/10.1021/op200239e | Org. ProcessRes. Dev. 2012, 16, 311−322

REFERENCES

(1) Broughton, D. B.; Gerhold, C. G. U.S. Patent 2,985,589 (A), 1961.
(2) Ruthven, D. M.; Ching, C. B. *Chem. Eng. Sci.* **1989**, *44*, 1011−1038.
(3) Juza, M.; Mazzotti, M.; Morbidelli, M. *Trends Biotechnol.* **2000**, *18*, 108−118.
(4) Rajendran, A.; Paredes, G.; Mazzotti, M. *J. Chromatogr., A* **2009**, *1216*, 709−738.
(5) Wankat, P. C. *Ind. Eng. Chem. Res.* **2001**, *40*, 6185−6193.
(6) Hur, J. S.; Wankat, P. C. *Ind. Eng. Chem. Res.* **2006**, *45*, 8713−8722.
(7) Kim, K. B.; Kishihara, S.; Fuji, S. *Biosci. Biotechnol. Biochem.* **1992**, *56*, 801−802.
(8) Wooley, R.; Ma, Z.; Wang, N. H. L. *Ind. Eng. Chem. Res.* **1998**, *37*, 3699−3709.
(9) Chiang, A. S. T. *AIChE J.* **1998**, *44*, 1930−1932.
(10) Kessler, L. C.; Seidel-Morgenstern, A. *J. Chromatogr., A* **2006**, *1126*, 323−337.
(11) Mun, S. *Ind. Eng. Chem. Res.* **2010**, *49*, 9258−9270.
(12) Hur, J. S.; Wankat, P. C. *Ind. Eng. Chem. Res.* **2005**, *44*, 1906−1913.
(13) Masuda, T.; Sonobe, T.; Matsuda, F.; Horie, M. U.S. Patent 5,198,120 (A), 1993.
(14) Mata, V. G.; Rodrigues, A. E. *J. Chromatogr., A* **2001**, *939*, 23−40.
(15) Aumann, L.; Morbidelli, M. *Biotechnol. Bioeng.* **2008**, *99*, 728−733.
(16) Paredes, G.; Abel, S.; Mazzotti, M.; Morbidelli, M.; Stadler, J. *Ind. Eng. Chem. Res.* **2004**, *43*, 6157−6167.
(17) Katsuo, S.; Mazzotti, M. *J. Chromatogr., A* **2010**, *1217*, 1354−1361.
(18) Katsuo, S.; Mazzotti, M. *J. Chromatogr., A* **2010**, *1217*, 3067−3075.
(19) Migliorini, C.; Mazzotti, M.; Morbidelli, M. *AIChE J.* **1999**, *45*, 1411−1421.
(20) Katsuo, S.; Langel, C.; Schanen, P.; Mazzotti, M. *J. Chromatogr., A* **2009**, *1216*, 1084−1093.
(21) Mazzotti, M.; Storti, G.; Morbidelli, M. *J. Chromatogr., A* **1997**, *769*, 3−24.
(22) Abel, S.; U. Bäbler, M.; Arpagaus, C.; Mazzotti, M.; Stadler, J. *J. Chromatogr., A* **2004**, *1043*, 201−210.
(23) Langel, C.; Grossmann, C.; Jermann, S.; Mazzotti, M.; Morari, M.; Morbidelli, M. *Ind. Eng. Chem. Res.* **2010**, *49*, 11996−12003.